Mechanical Systems and Signal Processing 83 (2017) 506–521

Contents lists available at ScienceDirect

Mechanical Systems and Signal Processing

journal homepage: www.elsevier.com/locate/ymssp

# A generalised multiple-mass based method for the determination of the live mass of a force transducer

Diogo Montalvão*, Thomas Baker, Balazs Ihracska, Muhammad Aulaqi

*School of Engineering and Technology, University of Hertfordshire, College Lane Campus, Hatfield AL10 9AB, United Kingdom*

ARTICLE INFO

*Article history:*
Received 20 July 2015
Received in revised form
10 June 2016
Accepted 16 June 2016
Available online 6 July 2016

*Keywords:*
Experimental Modal Analysis
Force transducer
Calibration
Live mass

ABSTRACT

Many applications in Experimental Modal Analysis (EMA) require that the sensors' masses are known. This is because the added mass from sensors will affect the structural mode shapes, and in particular its natural frequencies. EMA requires the measurement of the exciting forces at given coordinates, which is often made using piezoelectric force transducers. In such a case, the live mass of the force transducer, i.e. the mass as 'seen' by the structure in perpendicular directions must be measured somehow, so that compensation methods like mass cancelation can be performed. This however presents a problem on how to obtain an accurate measurement for the live mass. If the system is perfectly calibrated, then a reasonably accurate estimate can be made using a straightforward method available in most classical textbooks based on Newton's second law. However, this is often not the case (for example when the transducer's sensitivity changed over time, when it is unknown or when the connection influences the transmission of the force). In a self-calibrating iterative method, both the live mass and calibration factor are determined, but this paper shows that the problem may be ill-conditioned, producing misleading results if certain conditions are not met. Therefore, a more robust method is presented and discussed in this paper, reducing the ill-conditioning problems and the need to know the calibration factors beforehand. The three methods will be compared and discussed through numerical and experimental examples, showing that classical EMA still is a field of research that deserves the attention from scientists and engineers.
© 2016 The Authors. Published by Elsevier Ltd. This is an open access article under the CC BY license (http://creativecommons.org/licenses/by/4.0/).

## 1. Introduction

Piezoelectric force transducers operate with the principle that when a piezoelectric crystal is deformed by the action of a force, a charge output (proportional to the rate of change of the force acting on the crystal) is produced. As with piezoelectric accelerometers, force transducers can either be of the type 'charge' or IEPE (Integrated Electronics Piezo-Electric), depending if they bring built-in pre-amplifiers or not. IEPE transducers have built-in pre-amplifiers and thus do not need a charge amplifier in the measurement chain, as charge transducers do.

One example where force transducers are used is in the measurement of the Frequency Response Function (FRF) of a structure. The FRF contains information about the natural frequencies, modal damping factors and mode shapes of a structure. For harmonic (sinusoidal) excitation, the FRF is the relationship between the response and the force. If an

* Corresponding author.
*E-mail address:* d.montalvao@herts.ac.uk (D. Montalvão).

http://dx.doi.org/10.1016/j.ymssp.2016.06.028
0888-3270/© 2016 The Authors. Published by Elsevier Ltd. This is an open access article under the CC BY license (http://creativecommons.org/licenses/by/4.0/).

accelerometer is used, and as long as the excitation is harmonic, the amplitude of the FRF at a given frequency $\omega$ is:

$$H(\omega) = \frac{a(\omega)}{f(\omega)} \tag{1}$$

where $a(\omega)$ is the amplitude of the acceleration response to the amplitude of input force $f(\omega)$. Because this is a representation of the FRF that makes use of the acceleration, it is called "accelerance". For other types of excitation, autocorrelation functions may have to be used [1].

When measuring FRF data, one is concerned with the ratio of motion to force and not the individual values of any of these quantities [1]. Thus, it is possible to generate an excitation function, where force is transmitted to the structure using a shaker (Fig. 1). These excitation functions can be "Random", "Pseudo-Random", "Sweep-Sine", "Multi-Sine" or "Stepped-Sine" [1,2]. The push-rod shown (often also referred to as the "stinger" or "drive rod") is used to apply the excitation force from the shaker to the structure. The objective is to transmit controlled excitation to the structure in a given direction and, at the same time, to impose as little constraint on the structure as possible in all the other directions. The effects of the push-rod on EMA have been previously discussed, for example in [1,3–6].

Force transducers have a sandwich construction: a piezoelectric crystal is placed between a base case and a top case. Note that one side of the transducer may be lighter than the other. In a conventional force transducer setup and according to, e.g., [1,5], the transducer is placed with the lighter side (called the "base side") towards the structure and the heavy side (called the "top side") away from the structure (Fig. 2(a)). This is done to avoid as much mass modification to the structure as possible. The mass of the side that is attached to the structure is also called "live mass" [1,5]. This mass is 'seen' by the structure in the sensing direction. However, at perpendicular directions, the structure will 'see' the total mass of the force transducer. For example, these masses have been recorded as 3 g and 18 g on the different sides of a conventional force

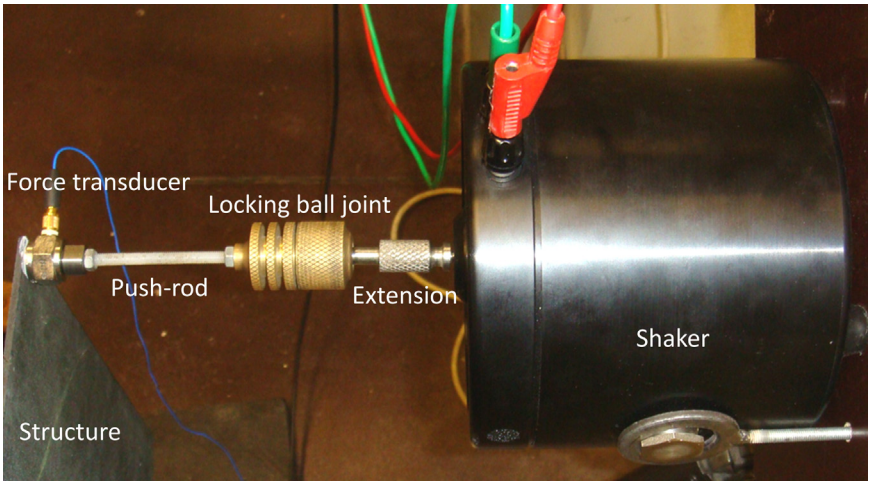


**Fig. 1.** Push-rod connection between a shaker and a force transducer [8].

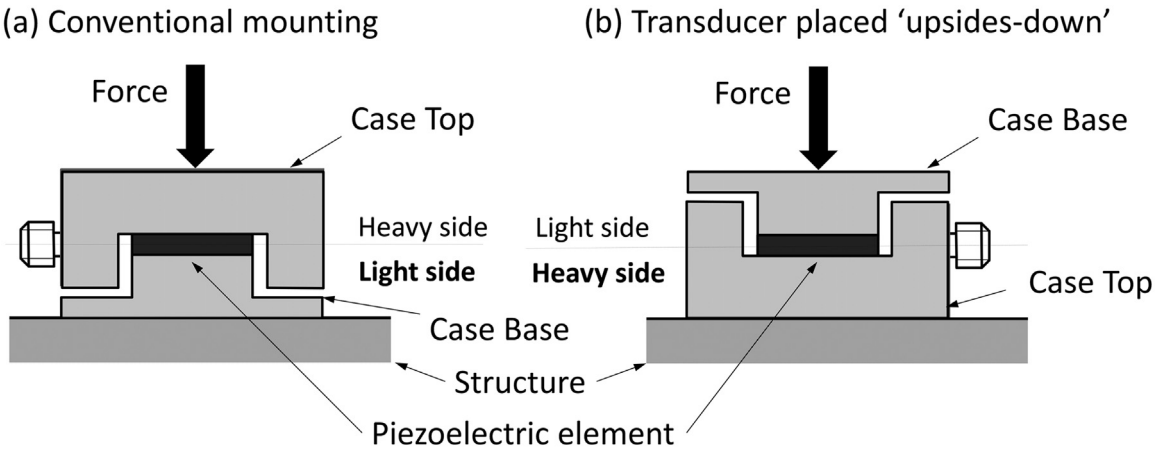


**Fig. 2.** Schematic cross-sectional view of a piezoelectric force transducer: (a) conventional mounting and (b) 'upsides-down' mounting.

transducer weighing a total of 21 g [1,5]. This of course would vary from one model to another, and even across different examples of the same model.

Note that the force transducer can also be attached with the heavier side on the side of the structure (Fig. 2(b)). In this case, the discrepancy between the live mass (18 g) and the mass 'seen' by the structure in perpendicular directions (21 g) will be smaller.

The live mass of a force transducer is important to know in many applications. For example, when mass cancellation procedures are put in place for accurate determination of the structural modal properties [1,3,7], the live mass of the force transducer is sometimes required. It is also important in FEM (Finite Element Model) validation and updating, especially when lightweight structures are concerned (e.g., composite structures) [8,9] or, for example, in methods that use a T-shaped block to determine the rotational terms of the FRF [1,10]. Mass-loading effects of transducers have been extensively studied before, for example in [1,3–7,11–17]. Because of these mass-loading effects, a rule of thumb is that the mass of the transducers should be at least less than 10% of the mass of the measured structure [18]. Other effects include stiffness and damping changes, for example due to the use of different tips when exciting the structure with an impact hammer. In this case, the different impact tips may also influence the measurement of the force (i.e., the sensitivity), as a consequence for example of using a rubber tip instead of a steel tip [19]. Considerations on other effects rather than the mass-loading effect at perpendicular directions (the live mass) will not be covered in this text.

The measurement of the live mass can be done by shaking a freely-suspended mass instrumented with a force transducer and a reference accelerometer with known mass [20,21]. This process is similar to a calibration procedure [1,19] where a pair of sensors composed of an accelerometer and force transducer is used. Based on Newton's Second law, the force experienced by the mass is simply the mass multiplied by the measured acceleration. Thus, it is possible to find a calibration correction factor based on the measurement of a known mass. Nevertheless, to do it properly requires the knowledge of the live mass at the same time, which typically is taken as an assumption. If, on the other hand, one wants to measure the live mass of the force transducer, then the system is assumed to be calibrated (i.e. the manufacturers' quoted sensitivities are considered to be accurate enough). This is not often the case as transducers' sensitivities may change with time and environmental conditions. Furthermore, in real circumstances where large structures are to be tested, long lead cables may change signal quality due to resistance, capacitance variation or noise pick-up [1].

In this paper, three methods to determine the live mass of a piezoelectric force transducer are presented and discussed, where two of the methods also allow determining the overall sensitivity of the measurement chain. The three methods are compared and discussed through numerical and experimental examples, so that the advantages and limitations of the methods can be thoroughly assessed.

## 2. Theoretical development

### 2.1. General equation

The classical method to determine the live mass of a force transducer starts with Newton's second law, which can be written as:

$$f = m \cdot a \tag{2}$$

The amplitude of the FRF as given by Eq. (1) thus becomes:

$$H(\omega) = \frac{a(\omega)}{f(\omega)} = \frac{1}{m} \tag{3}$$

It is very important to note that Eq. (3) is only valid within a limited low-frequency range where the whole system behaves as a pure rigid mass. Once the bodies start deforming elastically, it is no longer possible to relate the true value of the mass with the FRF as in Eq. (3). This is also why the inverse of Eq. (3) is often referred to as "apparent mass" or "inertance". Generically speaking, the inverse of the FRF $H(\omega)$ is called "mechanical impedance"[1] and is represented by $Z(\omega)$ [1]:

$$Z(\omega) = \frac{f(\omega)}{a(\omega)} = m^* \tag{4}$$

where $m^*$ denotes the apparent mass of the system (which should be the same as the mass of the system when it behaves rigidly, i.e. if the calibration factor is known). Eqs. (3) and (4) are correct only when the vibrating system is a single DOF system vibrating only in one direction, which is an assumption that will be made in the methods later proposed.

[1] The designation mechanical impedance actually suggests a relationship force/velocity. However, it is widely accepted as a general designation for any force/response relationship. In a similar way, mobility is accepted to be used to designate any form of the FRF 1.Maia, N.M.M. and J.M.M. e Silva, *Theoretical and experimental modal analysis*. 1997: Research Studies Press Taunton.

The mass in Eqs. (1), (3) and (4) is the total mass of the system, including the masses from the sensors. If one accelerometer is used and one force transducer is used, the apparent mass can be written as:

$$Z = m^* = m_f + m_k \tag{5}$$

where $m_f$ is the live mass of the force transducer and $m_k$ is the known mass of the system composed by the structure, accelerometer, mounting studs, etc. (all of which can can be measured on a weight scale). It is important to note that the total mass of the force transducer is not $m_f$. The live mass is just a portion of the total mass, depending on the force transducer's design. Likewise, the total mass of the force transducer is not considered when measuring the known mass $m_k$.

The correct measurement of the mechanical impedance depends on the calibration of the system. If the system is not calibrated (e.g. because the sensitivity of the transducers changed over time or because the calibration chart was lost) the obtained value for the mechanical impedance must be corrected by a correction factor, $\gamma$. In this case, and considering Eq. (5), Eq. (4) can be written as:

$$\gamma Z = m_f + m_k \tag{6}$$

where the dependency on frequency has been dropped for simplicity (if the structure is rigid, then the apparent mass is constant over frequency).

Eq. (6) is the basis for the three methods discussed and presented in this paper.

### 2.2. Single-Mass Based Method

In the single-mass based method, the measurement of one known mass is enough to determine the live mass of the force transducer. This method is based on the calibration method described in [1,19]. However, this method assumes that the system is calibrated: otherwise it is not possible to determine the live mass of the force transducer from the mechanical

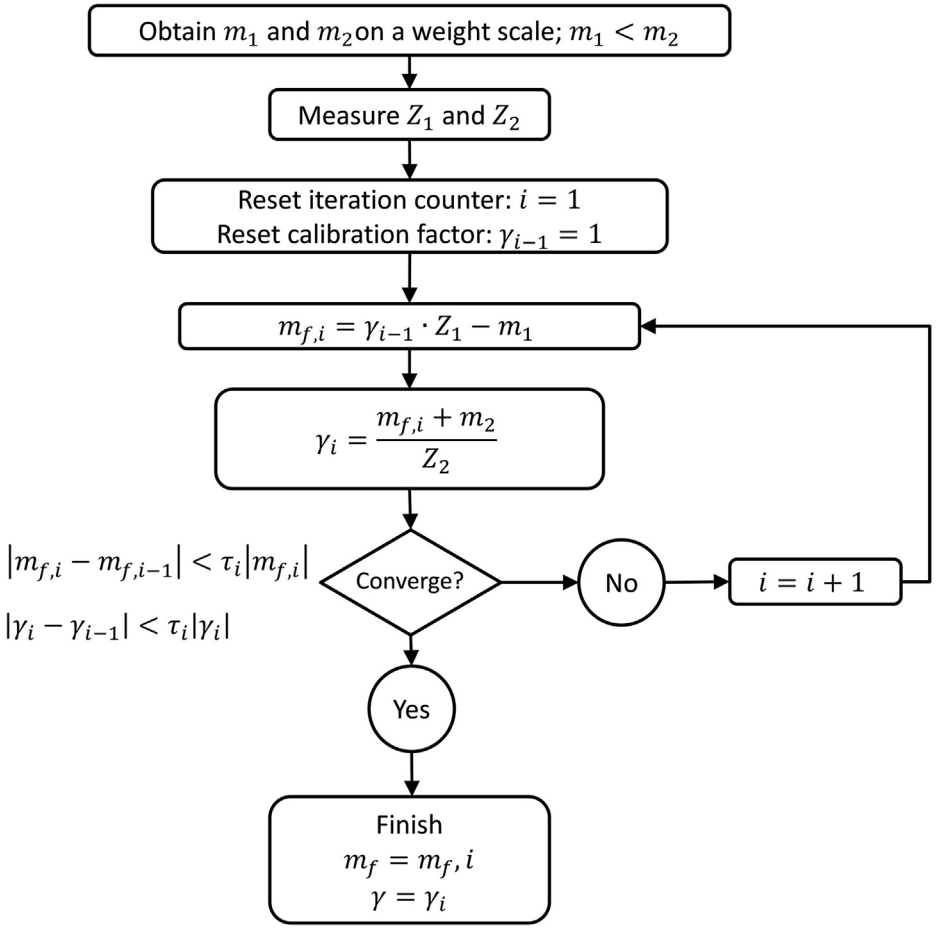


**Fig. 3.** Flowchart of the self-calibrating method proposed in [21] to determine the live mass of a force transducer.

impedance measurements, i.e.:

$$\gamma = 1 \tag{7}$$

Based on the assumption above (that the system is calibrated) and on Eq. (6), the live mass of the force transducer can therefore be determined from:

$$m_f = Z - m_k \tag{8}$$

### 2.3. Dual-Mass Based Method

Calibration of transducers may be necessary, for example because the sensitivity changed over time [1], because of sensitivity losses due to the stiffness at the attachment locations [12,19,22] or because of other reasons [6,15,17]. It might even happen that the calibration chart is missing. In the method described in [1] the calibration factor may be determined by rearranging Eq. (6) as follows:

$$\gamma = \frac{m_f + m_k}{Z} \tag{9}$$

However, this method for determining the sensitivity of the pair composed by accelerometer and force transducer assumes that the live mass of the force transducer is known beforehand. Either way, something must be assumed.

In an attempt to overcome the problem of having to know beforehand either the value of the live mass or the sensitivity factor, an iterative algorithm was developed [21] and used by [20,23] to determine both the live mass and the sensitivity factor from the measurements on two different masses, $m_1$ and $m_2$. The algorithm proposed by [21] can be described as a flow chart as in Fig. 3.

Because it is an iterative algorithm, it is not easy to implement. It is possible, however, to write equivalent expressions based on the same principle.

In this method, it is assumed that the live mass of the force transducer remains unchanged regardless of the mass of the total system. Similarly, it is assumed that the global sensitivity of the pair composed of the accelerometer and force transducer do not change from one measurement to the other. If we consider two different systems with known masses $m_1$ and $m_2$, Eq. (6) can be re-written for each system as:

$$\gamma = \frac{m_f + m_{k1}}{Z_1} \tag{10}$$

$$\gamma = \frac{m_f + m_{k2}}{Z_2} \tag{11}$$

By combining Eqs. (10) and (11) together and solving for $m_f$ one obtains:

$$m_f = \left(\frac{m_{k2}}{Z_2} - \frac{m_{k1}}{Z_1}\right) \cdot \left(\frac{1}{Z_1} - \frac{1}{Z_2}\right)^{-1} \tag{12}$$

The sensitivity factor can be determined from either Eqs. (10) or (11) once $m_f$ is known.

### 2.4. Multiple-Mass Based Method

One problem with the dual-mass based method is that it is ill-conditioned, as will be shown later. If the system is calibrated, if $m_{k1} \gg m_f$ and if $m_{k2} \gg m_f$, then the ratios $m_{k2}/Z_2$ and $m_{k1}/Z_1$ in Eq. (12) will approach 1. Thus, in that case, the difference in the numerator in Eq. (12) will be close to zero, or at least close to the order of magnitude of the error.

In an attempt to overcome the ill-conditioning problem from the dual-mass based method, a new method to determine the live mass of a force transducer and find the sensitivity factor is presented in this paper. This is also a general method that can make use of any number of different masses, starting at 2.

As in the dual-mass based method, it is assumed that the exact values of the calibration factor and live mass of the force transducer do not change between different tests, i.e., $\gamma_i = \gamma_j$ and $m_{fi} = m_{fj}$. If this would be the case, then:

$$\sum_{i=1}^{n}\sum_{j=1}^{n}(\gamma_i - \gamma_j)^2 = 0 \tag{13}$$

$$\sum_{i=1}^{n}\sum_{j=1}^{n}(m_{fi} - m_{fj})^2 = 0 \tag{14}$$

where

$$\gamma_i = \frac{m_f + m_{ki}}{Z_i}, \qquad \gamma_j = \frac{m_f + m_{kj}}{Z_j}, \qquad i = 1 \ldots n \tag{15}$$

$$m_{fi} = \gamma Z_i - m_{ki}, \qquad m_{fj} = \gamma Z_j - m_{kj}, \qquad i = 1 \ldots n \tag{16}$$

and $n$ is the number of different masses used in the system ($n \geq 2$).

However, it is known that the measurement of the live mass of the force transducer and the sensitivity factor may be polluted with experimental error. This means that it is hardly likely that Eqs. (13) and (14) are true propositions, since in reality $\gamma_i \neq \gamma_j$ and $m_{fi} \neq m_{fj}$, even if the differences are very small.

Thus, instead of solving for Eqs. (13) and (14), it is proposed that the problem is treated as a standard square minimum like optimization problem, where a cost function must be minimized, i.e.:

$$\frac{\mathrm{d}}{\mathrm{d}m_f}\left(\sum_{i=1}^{n}\sum_{j=1}^{n}(\gamma_i - \gamma_j)^2\right) = 0 \tag{17}$$

$$\frac{\mathrm{d}}{\mathrm{d}\gamma}\left(\sum_{i=1}^{n}\sum_{j=1}^{n}(m_{fi} - m_{fj})^2\right) = 0 \tag{18}$$

With these two Eqs. (17) and (18) it is possible to obtain one single value for the live mass of the force transducer and one single value for the global sensitivity of the pair composed by accelerometer and force transducer from any number of measurements with different known masses.

### 2.4.1. Multiple-Mass Based Method using two masses

If two masses are used, then Eqs. (15)–(18) become:

$$m_f = \frac{Z_1 m_{k2} - Z_2 m_{k1}}{Z_2 - Z_1} \tag{19}$$

$$\gamma = \frac{m_{k1} - m_{k2}}{Z_1 - Z_2} \tag{20}$$

which is equivalent to the dual-mass based method presented in Section 2.3. The advantage of writing Eq. (19) in the form of Eq. (12) presented earlier is that it highlights the ill-conditioning nature of determining the live mass from a system composed of two different masses only.

### 2.4.2. Multiple-Mass Based Method using three masses

If three masses are used, then Eqs. (17) and (18) become:

$$\frac{\mathrm{d}}{\mathrm{d}m_f}\left[(\gamma_1 - \gamma_2)^2 + (\gamma_1 - \gamma_3)^2 + (\gamma_2 - \gamma_3)^2\right] = 0 \tag{21}$$

$$\frac{\mathrm{d}}{\mathrm{d}\gamma}\left[(m_{f1} - m_{f2})^2 + (m_{f1} - m_{f3})^2 + (m_{f2} - m_{f3})^2\right] = 0 \tag{22}$$

Using Eqs. (15) and (16), the solutions for the live mass and sensitivity factor are, respectively:

$$\begin{aligned} m_f &= \frac{(a - 2d + b)m_{k3} + (a - 2e + c)m_{k2} + (b - 2f + c)m_{k1}}{2(d + e + f - a - b - c)} \\ a &= Z_1^2 Z_2 Z_3 \\ b &= Z_1 Z_2^2 Z_3 \\ c &= Z_1 Z_2 Z_3^2 \\ d &= Z_1^2 Z_2^2 \\ e &= Z_1^2 Z_3^2 \\ f &= Z_2^2 Z_3^2 \end{aligned} \tag{23}$$

$$\gamma = \frac{(-Z_1 - Z_2 + 2Z_3)m_{k3} + (-Z_1 + 2Z_2 - Z_3)m_{k2} + (2Z_1 - Z_2 - Z_3)m_{k1}}{2\left(Z_1^2 + Z_2^2 + Z_3^2 - Z_1 Z_2 - Z_1 Z_3 - Z_2 Z_3\right)} \tag{24}$$

When using three masses the method will be referred to as the triple-mass based method.

### 2.4.3. Multiple-mass based method with more than three masses

To extend the number of known masses to $n > 3$, the algebraic solutions of Eqs. (17) and (18) can become a challenge to determine. In this case, it is recommended that graphical or computational methods are used to find the minimum of the functions defined in Eqs. (13) and (14). These scenarios, however, will not be considered in this paper, although it is speculated that for an increased number of different masses, the accuracy in determining the live mass of the force transducer increases.

## 3. Numerical simulations

Numerical simulations were created in order to assess the three methods discussed in this paper. Different values for the added known masses have been considered, ranging from 10 g to 500 g. The live mass of the force transducer is 10 g. The experimental error was simulated by changing the sensitivity factors up to 5%. A total of 20 simulations, labelled A to T, are shown in Table 1. Results for the different three methods discussed in this paper are shown in Tables 2–4.

Case A is the ideal one where the system is perfectly calibrated, i.e., for the three different masses considered, the sensitivity of the measurement system is $\gamma_1 = \gamma_2 = \gamma_3 = 1$. As expected, under these circumstances, all the three methods

**Table 1**
Simulated data.

| Case | Simulated Sensitivity | | | Simulated Known Mass* | | | Simulated Apparent Mass** | | |
|---|---|---|---|---|---|---|---|---|---|
| | $\gamma_1$ | $\gamma_2$ | $\gamma_3$ | $m_{k1}$(g) | $m_{k2}$(g) | $m_{k3}$(g) | $Z_1$(g) | $Z_2$(g) | $Z_3$(g) |
| A | 1 | 1 | 1 | 10 | 100 | 500 | 20.0 | 110.0 | 510.0 |
| B | 1.05 | 1.05 | 1.05 | 10 | 100 | 500 | 19.0 | 104.8 | 485.7 |
| C | 1.05 | 1 | 1 | 10 | 100 | 500 | 19.0 | 110.0 | 510.0 |
| D | 1 | 1.05 | 1 | 10 | 100 | 500 | 20.0 | 104.8 | 510.0 |
| E | 1 | 1 | 1.05 | 10 | 100 | 500 | 20.0 | 110.0 | 485.7 |
| F | 1 | 1.05 | 1.05 | 10 | 100 | 500 | 20.0 | 104.8 | 485.7 |
| G | 1.05 | 1 | 1.05 | 10 | 100 | 500 | 19.0 | 110.0 | 485.7 |
| H | 1.05 | 1.05 | 1 | 10 | 100 | 500 | 19.0 | 104.8 | 510.0 |
| I | 1 | 1.025 | 1.05 | 10 | 100 | 500 | 20.0 | 107.3 | 485.7 |
| J | 1 | 1.05 | 1.025 | 10 | 100 | 500 | 20.0 | 104.8 | 497.6 |
| K | 1.025 | 1 | 1.05 | 10 | 100 | 500 | 19.5 | 110.0 | 485.7 |
| L | 1.025 | 1.05 | 1 | 10 | 100 | 500 | 19.5 | 104.8 | 510.0 |
| M | 1.05 | 1 | 1.025 | 10 | 100 | 500 | 19.0 | 110.0 | 497.6 |
| N | 1.05 | 1.025 | 1 | 10 | 100 | 500 | 19.0 | 107.3 | 510.0 |
| O | 1 | 1.025 | 1.05 | 250 | 100 | 500 | 260.0 | 107.3 | 485.7 |
| P | 1 | 1.05 | 1.025 | 250 | 100 | 500 | 260.0 | 104.8 | 497.6 |
| Q | 1.025 | 1 | 1.05 | 250 | 100 | 500 | 253.7 | 110.0 | 485.7 |
| R | 1.025 | 1.05 | 1 | 250 | 100 | 500 | 253.7 | 104.8 | 510.0 |
| S | 1.05 | 1 | 1.025 | 250 | 100 | 500 | 247.6 | 110.0 | 497.6 |
| T | 1.05 | 1.025 | 1 | 250 | 100 | 500 | 247.6 | 107.3 | 510.0 |

* The "simulated known mass" is an arbitrary number representing $m_k$ in Eq. (9). Hence, it does not include the live mass of the force transducer $m_f$.

** The "simulated apparent mass" is determined from $Z_i = \frac{m_f + m_{ki}}{\gamma_i}$, taking into account the simulated values for the sensitivity and apparent mass. In all cases it was arbitrarily chosen a value of 10 g for the live mass. For example, in case E where it is arbitrarily chosen for the simulation that $\gamma_3 = 1.05$ and $m_3 = 500$ g one obtains $Z_i = \frac{10+500}{1.05} = 487.5$ g.

**Table 2**
Results using simulated data (Single-Mass Based Method).

| Single-Mass Based Method | | | | | | |
|---|---|---|---|---|---|---|
| Case | $m_{f1}$(g) | $e_1$(%) | $m_{f2}$(g) | $e_2$(%) | $m_{f3}$(g) | $e_3$(%) |
| A | 10.0 | 0.0 | 10.0 | 0.0 | 10.0 | 0.0 |
| B | 9.0 | −9.5 | 4.8 | −52.4 | −14.3 | −242.9 |
| C | 9.0 | −9.5 | 10.0 | 0.0 | 10.0 | 0.0 |
| D | 10.0 | 0.0 | 4.8 | −52.4 | 10.0 | 0.0 |
| E | 10.0 | 0.0 | 10.0 | 0.0 | −14.3 | −242.9 |
| F | 10.0 | 0.0 | 4.8 | −52.4 | −14.3 | −242.9 |
| G | 9.0 | −9.5 | 10.0 | 0.0 | −14.3 | −242.9 |
| H | 9.0 | −9.5 | 4.8 | −52.4 | 10.0 | 0.0 |
| I | 10.0 | 0.0 | 7.3 | −26.8 | −14.3 | −242.9 |
| J | 10.0 | 0.0 | 4.8 | −52.4 | −2.4 | −124.4 |
| K | 9.5 | −4.9 | 10.0 | 0.0 | −14.3 | −242.9 |
| L | 9.5 | −4.9 | 4.8 | −52.4 | 10.0 | 0.0 |
| M | 9.0 | −9.5 | 10.0 | 0.0 | −2.4 | −124.4 |
| N | 9.0 | −9.5 | 7.3 | −26.8 | 10.0 | 0.0 |
| O | 10.0 | 0.0 | 7.3 | −26.8 | −14.3 | −242.9 |
| P | 10.0 | 0.0 | 4.8 | −52.4 | −2.4 | −124.4 |
| Q | 3.7 | −63.4 | 10.0 | 0.0 | −14.3 | −242.9 |
| R | 3.7 | −63.4 | 4.8 | −52.4 | 10.0 | 0.0 |
| S | −2.4 | −123.8 | 10.0 | 0.0 | −2.4 | −124.4 |
| T | −2.4 | −123.8 | 7.3 | −26.8 | 10.0 | 0.0 |

**Table 3**
Results using simulated data (Dual-Mass Based Method).

| Dual-Mass Based Method | | | | | | | | | |
|---|---|---|---|---|---|---|---|---|---|
| Case | $m_{f1,2}$(g) | $e$(%) | $m_{f1,3}$(g) | $e$(%) | $m_{f2,3}$(g) | $e$(%) | $\gamma_{1,2}$ | $\gamma_{1,3}$ | $\gamma_{2,3}$ |
| A | 10.0 | 0.0 | 10.0 | 0.0 | 10.0 | 0.0 | 1.000 | 1.000 | 1.000 |
| B | 10.0 | 0.0 | 10.0 | 0.0 | 10.0 | 0.0 | 1.050 | 1.050 | 1.050 |
| C | 8.8 | −11.5 | 9.0 | −9.9 | 10.0 | 0.0 | 0.990 | 0.998 | 1.000 |
| D | 11.2 | 12.4 | 10.0 | 0.0 | 3.4 | −65.9 | 1.062 | 1.000 | 0.987 |
| E | 10.0 | 0.0 | 11.0 | 10.4 | 17.1 | 71.1 | 1.000 | 1.052 | 1.065 |
| F | 11.2 | 12.4 | 11.0 | 10.4 | 10.0 | 0.0 | 1.062 | 1.052 | 1.050 |
| G | 8.8 | −11.5 | 10.0 | 0.0 | 17.1 | 71.1 | 0.990 | 1.050 | 1.065 |
| H | 10.0 | 0.0 | 9.0 | −9.9 | 3.4 | −65.9 | 1.050 | 0.998 | 0.987 |
| I | 10.6 | 6.1 | 11.0 | 10.4 | 13.4 | 34.4 | 1.031 | 1.052 | 1.057 |
| J | 11.2 | 12.4 | 10.5 | 5.2 | 6.7 | −33.2 | 1.062 | 1.026 | 1.018 |
| K | 9.4 | −5.9 | 10.5 | 5.1 | 17.1 | 71.1 | 0.995 | 1.051 | 1.065 |
| L | 10.6 | 6.0 | 9.5 | −5.1 | 3.4 | −65.9 | 1.056 | 0.999 | 0.987 |
| M | 8.8 | −11.5 | 9.5 | −5.0 | 13.5 | 35.3 | 0.990 | 1.024 | 1.032 |
| N | 9.4 | −5.8 | 9.0 | −9.9 | 6.6 | −34.0 | 1.020 | 0.998 | 0.993 |
| O | 5.4 | −45.7 | 38.0 | 279.7 | 13.4 | 34.4 | 0.982 | 1.108 | 1.057 |
| P | 1.2 | −87.7 | 23.6 | 136.1 | 6.7 | −33.2 | 0.966 | 1.052 | 1.018 |
| Q | 14.9 | 48.6 | 23.3 | 132.7 | 17.1 | 71.1 | 1.044 | 1.077 | 1.065 |
| R | 5.5 | −44.6 | −2.6 | −126.2 | 3.4 | −65.9 | 1.007 | 0.975 | 0.987 |
| S | 19.9 | 99.0 | −2.3 | −123.2 | 13.5 | 35.3 | 1.090 | 1.000 | 1.032 |
| T | 14.7 | 47.4 | −14.1 | −240.7 | 6.6 | −34.0 | 1.069 | 0.953 | 0.993 |

**Table 4**
Results using simulated data (Triple-Mass Based Method).

| Triple-Mass Based Method | | | |
|---|---|---|---|
| Case | $m_{f1,2,3}$(g) | $e$(%) | $\gamma_{1,2,3}$ |
| A | 10.0 | 0.0 | 1.000 |
| B | 10.0 | 0.0 | 1.050 |
| C | 9.0 | −10.5 | 0.999 |
| D | 10.4 | 4.1 | 0.996 |
| E | 10.7 | 6.8 | 1.056 |
| F | 11.1 | 11.1 | 1.051 |
| G | 9.6 | −4.1 | 1.054 |
| H | 9.3 | −6.5 | 0.995 |
| I | 10.9 | 9.0 | 1.054 |
| J | 10.8 | 7.6 | 1.024 |
| K | 10.1 | 1.2 | 1.055 |
| L | 9.9 | −1.3 | 0.995 |
| M | 9.3 | −7.3 | 1.026 |
| N | 9.2 | −8.5 | 0.997 |
| O | 11.6 | 15.6 | 1.061 |
| P | 5.4 | −46.1 | 1.021 |
| Q | 16.6 | 66.3 | 1.066 |
| R | 3.9 | −61.3 | 0.986 |
| S | 14.7 | 47.5 | 1.028 |
| T | 8.2 | −18.1 | 0.988 |

(single-mass, dual-mass and triple-mass based) produce an accurate estimate for the live mass of the force transducer, i.e., $m_f = 10$ g.

Case B still is an ideal case where, although the system is not perfectly calibrated, the sensitivity of the measurement chain does not change from one measurement to the next. Choosing an equal offset of 5% in the calibration factors, the sensitivities become $\gamma_1 = \gamma_2 = \gamma_3 = 1.05$. Case B shows that when the system is not perfectly calibrated the error on the measurement of the live mass of a force transducer can be quite considerable when using a single-mass based method (single-mass based method, Table 2). Also, the higher the known added mass, the higher the error for the same calibration factor. Thus, when following the single-mass based method to measure the live mass of a force transducer, it is desirable that the added mass is as low as possible in order to reduce error propagation when the sensitivity factor is not exactly one. However, if the calibration factor is not known, it is not possible to determine the live mass of the force transducer using the single-mass based method.

Cases C, D and E and F, G and H are cases where one sensitivity factor is different from the other two. The first observation from these 6 cases is that the dual-mass based method can become ill-conditioned when the two added masses used

are much larger than the live mass of the force transducer. This is because the ratios $m_{k2}/Z_2$ and $m_{k1}/Z_1$ in Eq. (12) will be close to 1. Thus, in this case, the difference in the numerator in Eq. (12) will be close to zero, or at least close to the order of magnitude of the error. The second observation is that, although ill-conditioning may occur, the dual-mass based method is much more robust than the single-mass based method, as it is less sensitive to changes in the calibration factors. Thus, when following the dual-mass based method to measure the live mass of a force transducer, it is desirable that one of the added masses is as low as possible in order to avoid ill-conditioning problems.

Cases I to N are cases where all the sensitivity factors from one measurement to the other differ in approximately 2.5%. The ill-conditioning problem still occurs in the dual-mass based method. However, the triple-mass based method seems to be much more robust than the dual-mass based method, regardless of the masses' values, as the maximum error verified between the determined value for the live mass and its true value was 11%. The maximum errors for the single-mass based method and dual-mass based method were 243% and 71%, respectively, for cases I to N. One interesting thing to note from the triple-mass based method is that the global sensitivity factor seems to be governed by the heaviest measurement's sensitivity factor. The same trend applies to the dual-mass based method.

Finally, cases O to T use the same sensitivities as cases I to N, except that all the three added masses are much larger (at least one order of magnitude) than the live mass of the force transducer. As expected, results deteriorate for both the dual-mass and triple-mass based methods, which suggests that both these methods are more accurate when at least one experiment is done with one of the added masses kept to a minimum value.

## 4. Experimental tests

### 4.1. Equipment Settings and Setups

Three different test setups were performed in different conditions in order to assess the experimental robustness of the three methods discussed (Fig. 4). In setup 1 the shaker and system are in the vertical position, with the shaker supported on the floor. In setup 2 the shaker is suspended from a crane and placed in the horizontal position with the transducers and added mass directly attached. In setup 3 the shaker and added mass are suspended in free-free simulated boundary conditions and a push-rod is used between the shaker and the force transducer.

The whole sensor and acquisition setup is a classical one used in EMA. A National Instruments (NI) data acquisition (DAQ) system was used. It consisted of a NI cDAQ-9174 USB-Chassis, a 24 bit NI 9234 Analog Input module and a NI 9263 Analog Output module. The data generation and acquisition software was programmed using LabVIEW 2013 from NI.

The test setup is the one shown in Fig. 4 earlier. The same accelerometer was used in all experiments, a pre-amplified miniature cubic PCB accelerometer type 333B30. The three force transducers tested were the following:

- PCB16 (PCB type 208C01, Serial no. LW34716) with a total mass of 23.5 g;
- PCB17 (PCB type 208C01, Serial no. LW34717) with a total mass of 23.5 g;
- BK (Brüel & Kjær type 8200) with a total mass of 21.7 g.

The first two PCB force transducers (PCB16 and PCB17) are pre-amplified, which means that they can be connected to the DAQ system directly. The Brüel & Kjær is a charge force transducer, so a charge amplifier had to be placed between the DAQ and the force transducer. The charge amplifier is considered to be a part of the force transducer in this case, as a change in its settings (sensitivity) will change the results.

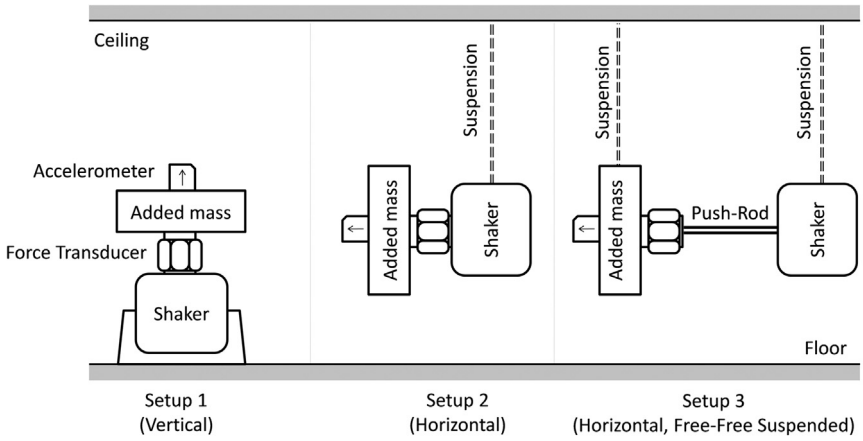


**Fig. 4.** Schematics of the three different test setups.

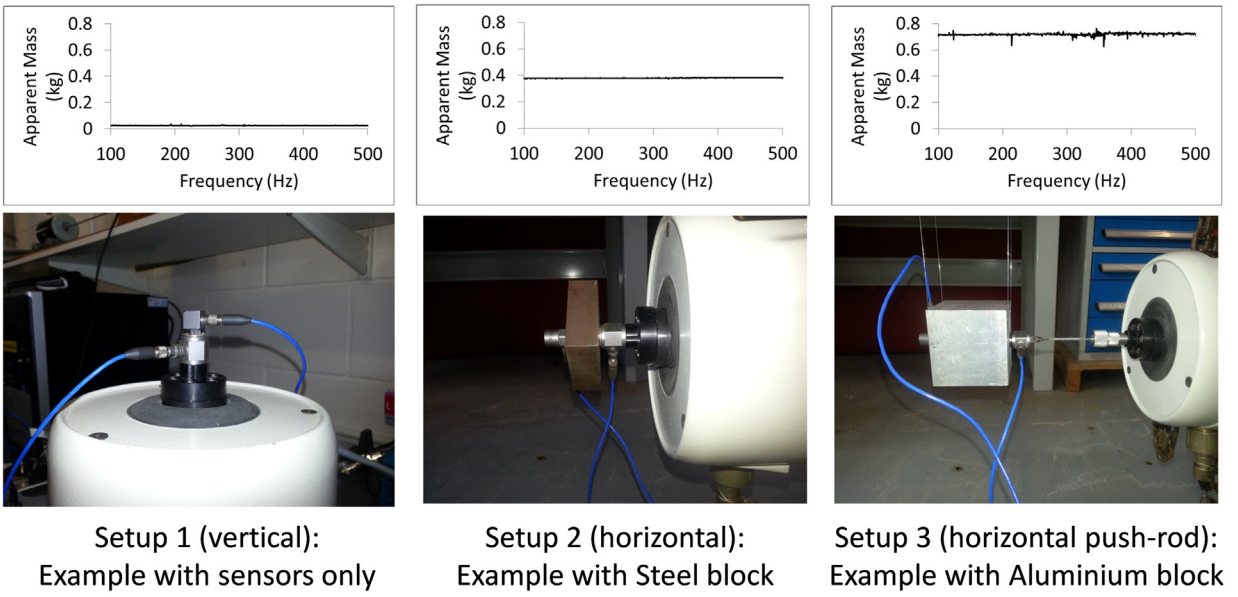


**Fig. 5.** Examples of the three test setups 1, 2 and 3 with different added masses and results in the 100–500 Hz frequency range: sensors only (0), steel block (St) and aluminium (Al) block. Example for the case when the PCB16 force transducer is used with its Base side on the structure's side.

The manufacturers' calibration factors were taken into consideration in the measurement system. However, in the case of the charge force transducer from Brüel & Kjær (BK), the charge amplifier settings were deliberately left unchanged (with the random values it presented at the time) in order to obtain a situation equivalent to one where the initial calibration factor is unknown or inadequately set. This can happen in a situation where the calibration chart for a particular transducer is not available or when its sensitivity changed over time.

A random excitation (white noise) and Hanning window were used with a frequency resolution of 0.5 Hz. The frequency range of interest was set from 100 Hz to 500 Hz so that the system behaves as a rigid body, i.e., the maximum frequency in the range is much lower than the first vibration mode. Any other frequency ranges could have been chosen, as long as this condition is met and there are enough data points in the sample. The shaker was a LDS V406 permanent magnet shaker connected to a LDS PA100E power amplifier.

### 4.2. Measurement of the apparent mass

To assess the robustness of the methods, three different added masses were considered: no added block (0), steel block (St) and aluminium block (Al). The total values of the known added masses include the mass from the block (when available), the total mass of the accelerometer, the masses of the mounting studs and an estimate of the mass of the connector on the accelerometer side (an existing damaged cable in the lab was cut from the connector and its weight was determined to be 1.5 g on a weight scale). Examples of the test setups with the corresponding results in the 100–500 Hz frequency range are shown in Fig. 5.

Fig. 5 shows that the frequency spectrum of the apparent mass may be affected by noise that may come from many different sources including a poor signal-to-noise ratio (but there may be many other sources). Although noise may have a deteriorating effect in the results, as long as it is random noise and not systematic, it is proposed that one of the following two ways are used in order to minimize its effect in determining the overall value of the apparent mass:

1. The overall value of the apparent mass is taken as the average of the data points in the frequency range of interest. The standard deviation gives a measure of the dispersion of data;
2. The overall value of the apparent mass is taken as the intersection at the origin of a linear fit to the data points. The slope should be as close to zero as possible, because the data points follow a constant trend. This is the approach used in this text.

### 4.3. Procedural guidelines

Whether the single-mass, dual-mass, triple-mass or any other multiple-mass based methods are chosen, the experimental procedure consists of determining, independently, pairs of values $(m_{ki}, Z_i)$ with $i = 1 \ldots n$ for a number $n$ of different masses. To obtain a pair of values $(m_{ki}, Z_i)$, the procedure is as follows:

**Table 5**
Experimental results – Setup 1 (vertical).

| Force Transducer | Side | Weighted Mass | | | Apparent Mass | | |
|---|---|---|---|---|---|---|---|
| | | System 0 $m_1$(g) | System St $m_2$(g) | System Al $m_3$(g) | System 0 $Z_1$(g) | System St $Z_2$(g) | System Al $Z_3$(g) |
| PCB16 | Base | 8 | 342.7 | 704.8 | 23.9 | 361.9 | 721.8 |
| PCB16 | Top | 8 | 342.7 | 704.8 | 17.1 | 336.3 | 732.4 |
| PCB17 | Base | 8 | 342.7 | 704.8 | 20.3 | 347.1 | 697.8 |
| PCB17 | Top | 8 | 342.7 | 704.8 | 19.0 | 350.6 | 686.8 |
| BK | Base | 9.3 | 344 | 706.1 | 21.6 | 510.1 | 1067.0 |
| BK | Top | 8 | 342.7 | 704.8 | 55.5 | 561.0 | 1072.2 |

**Table 6**
Experimental results – Setup 2 (horizontal).

| Force Transducer | Side | Weighted Mass | | | Apparent Mass | | |
|---|---|---|---|---|---|---|---|
| | | System 0 $m_1$(g) | System St $m_2$(g) | System Al $m_3$(g) | System 0 $Z_1$(g) | System St $Z_2$(g) | System Al $Z_3$(g) |
| PCB16 | Base | 8 | 342.7 | 704.8 | 23.3 | 375.8 | 777.0 |
| PCB16 | Top | 8 | 342.7 | 704.8 | 16.8 | 360.8 | 759.5 |
| PCB17 | Base | 8 | 342.7 | 704.8 | 20.3 | 368.7 | 771.0 |
| PCB17 | Top | 8 | 342.7 | 704.8 | 18.0 | 371.7 | 761.0 |
| BK | Base | 9.3 | 344 | 706.1 | 20.3 | 582.9 | 1188.2 |
| BK | Top | 8 | 342.7 | 704.8 | 45.3 | 596.8 | 1213.8 |

**Table 7**
Experimental results – Setup 3 (horizontal with push-rod).

| Force Transducer | Side | Weighted Mass | | | Apparent Mass | | |
|---|---|---|---|---|---|---|---|
| | | System 0 $m_1$(g) | System St $m_2$(g) | System Al $m_3$(g) | System 0 $Z_1$(g) | System St $Z_2$(g) | System Al $Z_3$(g) |
| PCB16 | Base | 8 | 342.7 | 704.8 | 23.3 | 340.3 | 712.2 |
| PCB16 | Top | 8 | 342.7 | 704.8 | 17.0 | 347.9 | 722.0 |
| PCB17 | Base | 8 | 342.7 | 704.8 | 20.3 | 345.7 | 713.5 |
| PCB17 | Top | 8 | 342.7 | 704.8 | 18.0 | 345.9 | 719.9 |
| BK | Base | 9.3 | 344 | 706.1 | 20.3 | 584.3 | 1196.7 |
| BK | Top | 8 | 342.7 | 704.8 | 45.3 | 615.5 | 1242.7 |

1. Decide on the method used[2] (number of masses), setting a value for $n$. For example, in the single-mass based method $n=1$, in the dual-mass based method $n=2$ and in the triple-mass based method $n=3$.
2. Measure the value of the $n$ different masses $m_{ki}$ ($i=1\ldots n$) on a calibrated weight scale[3]. Each $m_{ki}$ value should also include the mass of the accelerometer and any accessories required for the mounting.
3. It is suggested that the EMA setup is assembled in one of the forms presented in Section 4.1, but any other equivalent setups may be followed. For example, if setup 2 (horizontal) is followed, the shaker must first be suspended from the top. Next, the force transducer is attached to the shaker's armature, followed by the mass and the accelerometer (Fig. 4).
4. Using an appropriate excitation (e.g., random or multisine), determine the inverse of the accelerance (apparent mass or inertance) $Z_i$. This should be done only in the low frequency range where the system still behaves as a perfectly rigid body (i.e., before the first resonance).
5. If $n=1$ (single-mass based method), the value of the live mass may be determined from Eq. (8), assuming that the system is perfectly calibrated. Otherwise;
6. If $n\geq 2$, the system no longer needs to be calibrated. The live mass of the force transducer and sensitivity factor may be determined from Eqs. (17) and (18) for the general case where any number of masses are used. In the particular case where $n=2$ (dual-mass based), the algebraic solution given by Eqs. (19) and (20) can be used, whereas for $n=3$ (triple-mass based), Eqs. (23) and (24) are proposed.

[2] The single-mass based method ($n=1$) requires that the system is perfectly calibrated. It will also be shown that the method is very sensitive to the boundary conditions and magnitude of the added mass.

[3] As will be shown later, results for the live mass of the force transducer improve significantly when one of the added masses is very small when compared to the others. It is proposed that one of the systems is composed by the sensors alone (no added block).

The results for the pairs of values $(m_{ki}, Z_i)$ for the different setups, force transducers and added masses, are shown in Tables 5–7.

## 5. Experimental results

The live mass of the three force transducers was measured using the procedure discussed in the previous Sections 2 and 4. The three methods (single-mass, dual-mass and triple-mass based methods) were used on three different experimental test setups 1, 2 and 3 where the live mass was measured on either side of the force transducer. Three different added masses were used. When the method allowed it, the global sensitivity of the pair composed by accelerometer and force transducer was also determined (dual-mass and triple-mass based methods).

Since the exact values of the live masses are unknown on either side of the force transducer, one way to assess the quality of the experimental data is to compare the added value of the live masses on the base and top sides with the total mass of the force transducer. The total masses of the force transducers were measured on a weight scale and were determined to be 23.5 g for both the PCB force transducers and 21.7 g for the Brüel & Kjær force transducer.

### 5.1. Single-Mass Based Method

The values determined for the live mass on either side of the force transducers PCB16, PCB17 and BK in three different setups following the single-based mass method are shown in Tables 8–10.

### 5.2. Dual-Mass Based Method

The values determined for the live mass on either side of the force transducers PCB16, PCB17 and BK and the global sensitivities in three different setups following the dual-based mass method are shown in Tables 11–13.

### 5.3. Triple-Mass Based Method

The values determined for the live mass on either side of the force transducers PCB16, PCB17 and BK and the global sensitivities in three different setups following triple-based mass method are shown in Tables 14–16.

**Table 8**
Determining the live mass following the Single-Mass Based Method : Setup 1 (vertical).

| Force | Side | 0 | St | Al | Base+Top eff mass | | | % Error compared to total mass | | |
|---|---|---|---|---|---|---|---|---|---|---|
| Transducer | | $m_{f1}$ (g) | $m_{f2}$ (g) | $m_{f3}$ (g) | $m_{T1}$ (g) | $m_{T2}$ (g) | $m_{T3}$ (g) | $e_1$ (%) | $e_2$ (%) | $e_3$ (%) |
| PCB16 | Base | 15.9 | 19.2 | 17.0 | 24.9 | 12.8 | 44.5 | 6.1 | 46 | 89 |
| PCB16 | Top | 9.1 | −6.4 | 27.6 | | | | | | |
| PCB17 | Base | 12.3 | 4.4 | −7.0 | 23.2 | 12.3 | −24.9 | 1.1 | 48 | 206 |
| PCB17 | Top | 11.0 | 7.9 | −18.0 | | | | | | |
| BK | Base | 12.3 | 166.1 | 360.9 | 59.8 | 384.4 | 728.3 | 175 | 1672 | 3256 |
| BK | Top | 47.5 | 218.3 | 367.4 | | | | | | |

**Table 9**
Determining the live mass following the Single-Mass Based Method: Setup 2 (horizontal).

| Force | Side | 0 | St | Al | Base+Top eff mass | | | % Error compared to total mass | | |
|---|---|---|---|---|---|---|---|---|---|---|
| Transducer | | $m_{f1}$ (g) | $m_{f2}$ (g) | $m_{f3}$ (g) | $m_{T1}$ (g) | $m_{T2}$ (g) | $m_{T3}$ (g) | $e_1$ (%) | $e_2$ (%) | $e_3$ (%) |
| PCB16 | Base | 15.3 | −2.4 | 7.4 | 24.3 | 2.8 | 24.6 | 3.4 | 88 | 5 |
| PCB16 | Top | 9.0 | 5.2 | 17.2 | | | | | | |
| PCB17 | Base | 12.3 | 3.0 | 8.7 | 22.3 | 6.2 | 23.7 | 4.9 | 74 | 1 |
| PCB17 | Top | 10.0 | 3.2 | 15.1 | | | | | | |
| BK | Base | 11.0 | 240.3 | 490.6 | 48.4 | 513.0 | 1028.5 | 123 | 2264 | 4640 |
| BK | Top | 37.3 | 272.8 | 537.9 | | | | | | |

**Table 10**
Determining the live mass following the Single-Mass Based Method: Setup 3 (horizontal with push-rod).

| Force | Side | 0 | St | Al | Base + Top eff mass | | | % error compared to total mass | | |
|---|---|---|---|---|---|---|---|---|---|---|
| Transducer | | $m_{f1}$ (g) | $m_{f2}$ (g) | $m_{f3}$ (g) | $m_{T1}$ (g) | $m_{T2}$ (g) | $m_{T3}$ (g) | $e_1$ (%) | $e_2$ (%) | $e_3$ (%) |
| PCB16 | Base | 15.3 | 33.1 | 72.2 | 24.1 | 51.2 | 126.9 | 2.6 | 118 | 440 |
| PCB16 | Top | 8.8 | 18.1 | 54.7 | | | | | | |
| PCB17 | Base | 12.3 | 26.0 | 66.2 | 22.3 | 55.0 | 122.4 | 4.9 | 134 | 421 |
| PCB17 | Top | 10.0 | 29.0 | 56.2 | | | | | | |
| BK | Base | 11.0 | 238.9 | 482.1 | 48.4 | 493.0 | 991.1 | 123 | 2172 | 4467 |
| BK | Top | 37.3 | 254.1 | 509.0 | | | | | | |

**Table 11**
Determining the live mass and global sensitivity following the dual-mass based method: Setup 1 (vertical).

| Force | Side | 0-St | | 0-Al | | St-Al | | Base + Top eff mass | | | % Error compared to total mass | | |
|---|---|---|---|---|---|---|---|---|---|---|---|---|---|
| Transducer | | $m_{f1,2}$ (g) | $\gamma_{f1,2}$ | $m_{f1,3}$ (g) | $\gamma_{f1,3}$ | $m_{f2,3}$ (g) | $\gamma_{f1,3}$ | $m_{T1,2}$ (g) | $m_{T1,3}$ (g) | $m_{T2,3}$ (g) | $e_{1,2}$ (%) | $e_{1,3}$ (%) | $e_{2,3}$ (%) |
| PCB16 | Base | 15.6 | 0.990 | 15.8 | 0.998 | 21.5 | 1.006 | 25.5 | 24.4 | -13.8 | 8.6 | 4.0 | 159 |
| PCB16 | Top | 9.9 | 1.049 | 8.6 | 0.974 | −35.3 | 0.914 | | | | | | |
| PCB17 | Base | 12.8 | 1.024 | 12.9 | 1.028 | 15.6 | 1.032 | 23.9 | 24.6 | 50.5 | 1.8 | 4.9 | 115 |
| PCB17 | Top | 11.1 | 1.009 | 11.8 | 1.043 | 34.8 | 1.077 | | | | | | |
| BK | Base | 5.5 | 0.685 | 5.1 | 0.667 | −12.3 | 0.650 | 34.2 | 35.1 | 42.4 | 58 | 62 | 95 |
| BK | Top | 28.7 | 0.662 | 30.0 | 0.685 | 54.7 | 0.708 | | | | | | |

**Table 12**
Determining the live mass and global sensitivity following the dual-mass based method: Setup 2 (horizontal).

| Force | Side | 0-St | | 0-Al | | St-Al | | Base + Top eff mass | | | % Error compared to total mass | | |
|---|---|---|---|---|---|---|---|---|---|---|---|---|---|
| Transducer | | $m_{f1,2}$ (g) | $\gamma_{f1,2}$ | $m_{f1,3}$ (g) | $\gamma_{f1,3}$ | $m_{f2,3}$ (g) | $\gamma_{f1,3}$ | $m_{T1,2}$ (g) | $m_{T1,3}$ (g) | $m_{T2,3}$ (g) | $e_{1,2}$ (%) | $e_{1,3}$ (%) | $e_{2,3}$ (%) |
| PCB16 | Base | 16.6 | 1.056 | 15.5 | 1.011 | −11.4 | 0.974 | 25.8 | 24.4 | −17.3 | 9.8 | 3.7 | 173 |
| PCB16 | Top | 9.2 | 1.011 | 8.8 | 0.988 | −5.9 | 0.968 | | | | | | |
| PCB17 | Base | 12.9 | 1.028 | 12.4 | 1.005 | −2.3 | 0.985 | 23.3 | 22.3 | −10.1 | 0.9 | 5.0 | 143 |
| PCB17 | Top | 10.4 | 1.021 | 9.9 | 0.993 | −7.9 | 0.968 | | | | | | |
| BK | Base | 2.8 | 0.594 | 2.7 | 0.592 | 1.5 | 0.591 | 21.4 | 21.1 | 14.1 | 1 | 3 | 35 |
| BK | Top | 18.6 | 0.587 | 18.4 | 0.582 | 12.6 | 0.577 | | | | | | |

**Table 13**
Determining the live mass and global sensitivity following the dual-mass based method: Setup 3 (horizontal with push-rod).

| Force | Side | 0-St | | 0-Al | | St-Al | | Base + Top eff mass | | | % Error compared to total mass | | |
|---|---|---|---|---|---|---|---|---|---|---|---|---|---|
| Transducer | | $m_{f1,2}$ (g) | $\gamma_{f1,2}$ | $m_{f1,3}$ (g) | $\gamma_{f1,3}$ | $m_{f2,3}$ (g) | $\gamma_{f1,3}$ | $m_{T1,2}$ (g) | $m_{T1,3}$ (g) | $m_{T2,3}$ (g) | $e_{1,2}$ (%) | $e_{1,3}$ (%) | $e_{2,3}$ (%) |
| PCB16 | Base | 14.1 | 0.949 | 13.5 | 0.924 | −3.5 | 0.903 | 22.5 | 21.3 | −18.6 | 4.3 | 9.3 | 179 |
| PCB16 | Top | 8.4 | 0.973 | 7.8 | 0.938 | −15.1 | 0.908 | | | | | | |
| PCB17 | Base | 11.5 | 0.961 | 10.8 | 0.928 | −10.8 | 0.900 | 20.6 | 19.8 | −7.8 | 12.5 | 15.9 | 133 |
| PCB17 | Top | 9.1 | 0.946 | 8.9 | 0.938 | 3.1 | 0.930 | | | | | | |
| BK | Base | 2.8 | 0.595 | 2.8 | 0.597 | 4.7 | 0.598 | 22.3 | 21.9 | 12.3 | 3 | 1 | 43 |
| BK | Top | 19.5 | 0.607 | 19.0 | 0.596 | 7.5 | 0.587 | | | | | | |

## 6. Discussion of experimental results

The experimental results shown in Tables 8–16 highlight the same findings from the numerical simulations (Tables 2–4), which are:

1. The single-mass based method requires that the transducers' calibration factors are known beforehand. This can be seen from the results obtained with the BK force transducer where the sensitivity used was not the correct one, yielding results for the total mass obtained from the sum of the masses on either side of the force transducer very different from the one obtained on a weight scale.
2. The dual-mass based method is ill-conditioned when the added masses are much larger than the live mass of the force transducer. This can be seen from the pair of results obtained using the Steel and Aluminium block.

**Table 14**
Determining the live mass and global sensitivity following the triple-mass based method: Setup 1 (vertical).

| Force | Side | 0-St-Al | | Base + Top eff mass | % Error compared to total mass |
|---|---|---|---|---|---|
| Transducer | | $m_{f1,2,3}$ (g) | $\gamma_{f1,2,3}$ | $m_{T1,2,3}$ (g) | $e_{1,2,3}$ (%) |
| PCB16 | Base | 15.7 | 0.998 | 25.0 | 6.2 |
| PCB16 | Top | 9.2 | 0.972 | | |
| PCB17 | Base | 12.8 | 1.028 | 24.3 | 3.4 |
| PCB17 | Top | 11.5 | 1.043 | | |
| BK | Base | 5.3 | 0.666 | 34.7 | 60 |
| BK | Top | 29.5 | 0.685 | | |

**Table 15**
Determining the live mass and global sensitivity following the triple-mass based method: Setup 2 (horizontal).

| Force | Side | 0-St-Al | | Base + Top eff mass | % Error compared to total mass |
|---|---|---|---|---|---|
| Transducer | | $m_{f1,2,3}$ (g) | $\gamma_{f1,2,3}$ | $m_{T1,2,3}$ (g) | $e_{1,2,3}$ (%) |
| PCB16 | Base | 16.0 | 1.010 | 25.0 | 6.5 |
| PCB16 | Top | 9.0 | 0.988 | | |
| PCB17 | Base | 12.6 | 1.005 | 22.8 | 3.1 |
| PCB17 | Top | 10.1 | 0.992 | | |
| BK | Base | 2.8 | 0.592 | 21.2 | 2 |
| BK | Top | 18.5 | 0.582 | | |

**Table 16**
Determining the live mass and global sensitivity following the triple-mass based method: Setup (horizontal with push-rod).

| Force | Side | 0-St-Al | | Base + Top eff mass | % Error compared to total mass |
|---|---|---|---|---|---|
| Transducer | | $m_{f1,2,3}$ (g) | $\gamma_{f1,2,3}$ | $m_{T1,2,3}$ (g) | $e_{1,2,3}$ (%) |
| PCB16 | Base | 13.8 | 0.924 | 21.9 | 7.0 |
| PCB16 | Top | 8.1 | 0.937 | | |
| PCB17 | Base | 11.2 | 0.928 | 20.1 | 14.3 |
| PCB17 | Top | 9.0 | 0.938 | | |
| BK | Base | 2.8 | 0.597 | 22.1 | 2 |
| BK | Top | 19.3 | 0.596 | | |

3. Although the triple-mass based method showed to be less sensitive than the dual-mass based method, both measurement techniques may provide sufficiently accurate estimates of the live mass of a force transducer if one of the measurements is made using a very small added mass. The value for the global sensitivity depends more on the heaviest added mass measurement, because the relative transducers' added mass effect is smaller.

Besides these findings, the experimental results also allow drawing other important conclusions:

4. The BK values from setups 2 and 3 (horizontal setups where shaker is suspended) show evidence that the live mass of the force transducer was estimated with accuracy. It has been earlier reported [1,5] that the base mass of a similar force transducer is 3 g and the top mass is 18 g. For example, the results obtained in Table 16 for setup 2 show values of 2.8 g and 18.5 g for the base and top mass of the BK force transducer respectively. In other works, the value for the top side was determined to be 19.7 g [21] and the values for the base and top side were determined to be 17.1 g and 10.1 g respectively [20] for the same force transducer's model and using the dual-mass based method. It is important to note that, in this work and contrary to [20,21], the cable's connector on the side of the accelerometer was taken into account in the weighed mass with a value of 1.5 g, otherwise the estimated values for the live masses would have been slightly different.
5. Since the PCB16 and PCB17 setups used the correct calibration factors from the manufacturers, it would be expected that the global sensitivities using these transducers would be close to one. On one hand, when comparing the triple-mass based method between setups 2 and 3 (Tables 15 and 16), setup 2 (horizontal position with the masses and sensors directly attached to the shaker) is the one where the global sensitivity factors for both PCB16 and PCB17 force transducers are closer to one. However, setup 2 also presents the largest discrepancies between the base side mass of force transducers PCB16 and PCB17, which were determined to be 16.0 g and 12.6 g respectively. Setup 3 (horizontal free-free suspended configuration with push-rod) presents more consistent estimates for these values, with 13.8 g and 11.2 g respectively. On the top side, setup 2 produced 9.0 g and 10.1 g for the PCB16 and PCB17 force transducers respectively,

whereas setup 3 produced 8.1 g and 9.0 g for the PCB16 and PCB17 force transducers respectively. First of all, it is not guaranteed that the global sensitivity factors have not in fact changed over time or been influenced by other factors, like environmental conditions or the setup itself, which may be the reason why setup 3 may be presenting global sensitivity factors slightly lower than one. On the other hand, this may well be because each force transducer is a unique sensor, in what each one has its own sensitivity and frequency response curves. Thus, it is reasonable to assume that the live masses may also differ from one transducer to the other, even within the same model.

6. The previous point is reinforced from the fact that the single-mass based method, that considers the system to be well calibrated, produced consistent results between setups 2 and 3 for both force transducers PCB16 and PCB17.
7. The fact that the global sensitivities vary from one measurement to another is most likely related to experimental uncertainty and noise rather than anything else. There also is the rest of the measurement chain, composed by cables, connectors and the DAQ system itself, which may contribute to these differences as well. In certain circumstances cables may have a strong influence in the results [8], even when pre-amplified transducers are used, because they also add mass and stiffness to the system in an unpredictable way.
8. The test setup plays a decisive role in the outcome. Setup 1 (vertical position with shaker placed on the floor) produced the largest errors when comparing the total mass obtained from the sum of the masses on either side of the force transducer and the one obtained on a weight scale. First of all, setup 1 may introduce a reaction force at the base of the shaker that cannot be estimated, due to the uncertainty in the boundary conditions. Furthermore, if the shaker is placed on a soft foundation, for example a wooden table, this may introduce additional sources of vibration that could even be in other directions rather than the longitudinal alone. However, even when the shaker is freely suspended at the horizontal position as in setup 2, the direct attachment of the force transducer to the shaker's armature can cause distortions through secondary forces and/or moments in test results due to the exciter's inertial rigidity. However, even when a flexible push-rod is employed as in setup 3, errors can occur due to the force transducer's bending moment sensitivity [6]. While this was in fact expected, both setups 2 and 3 seem to provide the most reliable estimates for the base and top masses of the force transducers, since these setups reduce the influence of the boundary conditions on the experimental results.
9. It is interesting to note that there might not be consensus about which side on the force transducer has the largest mass. The BK force transducer does not show which one is the base or top side, whereas both the PCB16 and PCB17 have it written on its casing. Thus, for the BK force transducer the base side was considered to be the one with the smallest mass, following [1,5] where it is said that a force transducer is constructed to have a little mass on the base side of the sensing element as little as possible. However, as it can be seen from the results, the PCB force transducers are constructed in the exact opposite way, showing a smaller value on the top side and a larger one on the base side.
10. It can be seen that the live mass can be determined using either the dual-mass or the triple-mass based methods when one measurement is made with a small mass, even if the global sensitivity is unknown, as depicted from the BK results where the global sensitivity factors are determined to be 0.6 approximately.

## 7. Conclusion

This paper deals with the measurement of the live mass of force transducers for applications in EMA, using a combination of different calibration masses. Also, three methods are presented and discussed, where a different number of calibration masses are used.

The main conclusion is that the fact that at least two masses are used allows obtaining a reliable value for the live mass of the force transducer and calibration factor for the whole measurement chain. This is true when at least when one of the added calibration masses is very small in value. However, when such a situation is difficult to implement, the use of more calibration masses may lead to increased accuracy. A generalised method is presented in this paper, which allows, in theory, for any amount of calibration masses to be used.

Numerical and experimental tests show that results are consistent and that there is good agreement with existing literature and technical aspects on the construction of force transducers. The test setups are fully described and only require vibration equipment that is usually readily available for researchers and engineers working in the field. Besides providing a sustained estimate for the value of the live mass of the force transducer, tests are fast and simple to implement.

## Acknowledgments

The authors deny any conflicts of interest. This research received no specific grant from any funding agency in the public, commercial, or not-for-profit sectors.

## References


[1] N.M.M. Maia, J.M.M. e Silva, Theoretical and Experimental Modal Analysis, Research Studies Press, Taunton, 1997.
[2] D., Montalvão, M. Fontul, Harmonica: Stepped-Sine Spectrum Analyser for Transfer Function Measurement and Non-Linear Experimental Assessment, in Proceedings of M2D'2006 - 5th International Conference on Mechanics and Materials in Design. 2005: Porto, Portugal. Paper no. A0519.0506.
[3] D. Ewins, Modal Testing: Theory and Practice, Research Studies Press Ltd, Hertfordshire, 1984.
[4] X. Hu, Effects of Stinger Axial Dynamics and Mass Compensation Methods on Experimental Modal Analysis, Iowa State University, Ames, Iowa, 1992.
[5] J. Wright, G. Skingle. On the direct or indirect measurement of force in vibration-testing, in: Proceedings of SPIE, the International Society for Optical Engineering. 1997. Society of Photo-Optical Instrumentation Engineers.
[6] K. McConnell, P. Varoto. Force transducer bending moment sensitivity can affect the measured frequency response functions, in: Proceedings of the 11th International Modal Analysis Conference (IMAX XI). 1993. SEM Society for Experimental Mechanics Inc.
[7] J. Silva, N. Maia, A. Ribeiro, Cancellation of mass-loading effects of transducers and evaluation of unmeasured frequency response functions, J. Sound Vibr. 236 (5) (2000) 761–779.
[8] D. Montalvão, A modal-based contribution to damage location in laminated composite plates, in: Mechanical Engineering Department. 2010, Ph.D. dissertation, Instituto Superior Técnico, Technical University of Lisbon.
[9] D. Montalvão, et al., An experimental study on the evolution of modal damping with damage in carbon fiber laminates, J. Compos. Mater. (2014)., p. 0021998314547526.
[10] D. Montalvao, et al., Estimation of the rotational terms of the dynamic response matrix, Shock Vibr. 11 (3-4) (2004) 333–350.
[11] M. Ashory, Correction of mass-loading effects of transducers and suspension effects in modal testing, in: Proceedings of the 16th Modal Analysis Conference (IMAC XVI), Society of Photo-Optical Instrumentation Engineers, Santa Barbara, California, 1998.
[12] N. Baldanzini, M. Pierini, An assessment of transducer mass loading effects on the parameters of an experimental statistical energy analysis (SEA) model, Mech. Syst. Signal Process. 16 (5) (2002) 885–903.
[13] S. Bi, et al., Elimination of transducer mass loading effects in shaker modal testing, Mech. Syst. Signal Process. 38 (2) (2013) 265–275.
[14] A. Karle, S. Bhoite, A. Amale, Investigation of transducer mass loading effect in Frequency Response Function (FRF), Int. J. Emerg. Trends Sci. Technol. 1 (2014) 04.
[15] K.G. McConnell, The interaction of force transducers with their test environment, Int. J. Anal. Exp. Modal Anal. 8 (1993) 137–149.
[16] O. Dossing, Prediction of transducer mass-loading effects and identification of dynamic mass. in Proceedings of the 9th International Modal Analysis Conference (IMAX IX). 1991.
[17] N. Medina, J. de Vicente, Force sensor characterization under sinusoidal excitations, Sensors 14 (10) (2014) 18454–18473.
[18] P.L. Gatti, Applied Structural and Mechanical Vibrations: Theory and Methods, CRC Press, Boca Raton, Florida, 2014.
[19] T. Wang, et al. Practical calibration techniques for the modal impact hammer, In: Proceedings of the 34th International Modal Analysis Conference (IMAC XXXIV), Sensors and Instrumentation, Volume 5, Springer, Orlando, Florida, 2015, 23–29.
[20] J. Arina, Análise da Complementaridade dos Critérios para a Localização de Dano em Placas de Compósitos Laminados, in Mechanical Engineering Department. 2012, MSc dissertation, Instituto Superior Técnico, Technical University of Lisbon.
[21] D. Montalvão, Determination of Rotational Terms of the Dynamic Response by Means of Modal Analysis Techniques, in Mechanical Engineering Department. 2003, MSc dissertation, Instituto Superior Técnico, Technical University of Lisbon.
[22] C. Schlegel, et al., Sinusoidal calibration of force transducers using electrodynamic shaker systems, Sens. Transducers 14 (1) (2012) 95.
[23] M. Aulaqi, A self-calibrating technique to find the active mass on a force transducer, in School of Engineering and Technology. 2015, B. Eng project, University of Hertfordhshire.